Int. J. Heat Mass Transfer. Vol. 25, No. 11, pp. 1725–1735, 1982
Printed in Great Britain

0017–9310/82/111725–11 $03.00/0

AEROSOL AND GAS DEPOSITION TO FULLY ROUGH SURFACES: FILTRATION MODEL FOR BLADE-SHAPED ELEMENTS

J. FERNANDEZ DE LA MORA* and S. K. FRIEDLANDER

Department of Chemical Engineering and Center for Intermedia Research,
UCLA, Los Angeles, CA 90024, U.S.A.

(*Received* 25 *January* 1982 *and in final form* 5 *April* 1982)

Abstract—Rates of particle and gas transport to rough surfaces from turbulent flows can be related to the collection efficiencies of the individual roughness elements. Transport to the fully rough surfaces is rapid so the (average) concentration is nearly constant from the main flow into the roughness layer, and the rate limiting step is deposition to the roughness elements. Expressions for the deposition rate can be derived using filtration theory, modified to take into account the high Reynolds number flow around the elements. Data from the literature on particle and gas transport to blades of artificial grass can be correlated using the nondimensional variables of filtration theory. The correlation is satisfactory over more than nine orders of magnitude of the deposition variable and shows proper limiting forms in the small and large particle size ranges.

NOMENCLATURE

B^{-1}, difference between the transfer coefficient for mass and momentum to the roughness sublayer, $w(h)_\rho u_*/j'' - u(b)/u_*$;
b, constant defined by equation (3.32);
b', constant in equation (2.1), equal to 0.2 [6];
d_p, particle diameter [μm];
D, particle diffusion coefficient [$cm^2\,s^{-1}$];
f, stream function giving stagnation region velocity field;
f', f'', first and second derivatives of f respect to η;
F, nondimensional particle density, equation (3.20);
g, gravitational acceleration [$cm\,s^{-2}$];
G, constant in equation (2.14);
h, characteristic height of individual protrusions [cm];
h^+, nondimensional height, hu_*/ν;
j'', mass flux [$g\,cm^{-2}\,s^{-1}$];
k, defined by equation (3.7);
k_s, equivalent sand roughness;
K, effective rate constant defined in equation (2.4) [s^{-1}]; in equations (3.10) and (3.11) it describes the variation of the stream function with X away from the stagnation point;
K', defined by equation (3.13);
m, integer number in equation (3.31);
n, particle density [$g\,cm^{-3}$];
n_e, free stream value of n, equation (3.18) [$g\,cm^{-3}$];
Pr, Prandtl number, or ratio between the carrier gas kinematic viscosity and the diffusivity D (or the heat diffusivity for heat transfer). For mass transfer problems the Schmidt number Sc is generally employed instead of Pr;
Q, defined by equation (2.9);
r_p, particle radius [μm];
R, characteristic length of the obstacle's cross-section. For the artificial grass of refs. [5, 8] ($R = 0.5$ cm) it is the blade width [cm];
Re, Reynolds number for the flow around the obstacle, RU_∞/ν;
S, vertical area of protrusions available per unit volume for deposition [cm^{-1}];
u, mean velocity along the flow direction [$cm\,s^{-1}$];
u_*, turbulent friction velocity based on the wall shear τ_w and the fluid density ρ, $(\tau/\rho)^{1/2}$ [$cm\,s^{-1}$];
U, fluid velocity within the boundary layer of a single cylindrical fiber in the direction parallel to the wall, equation (3.1) [$cm\,s^{-1}$];
U_∞, velocity far from the single fiber in the flow direction [$cm\,s^{-1}$];
v_g, particle deposition velocity, reported in ref. [5] [$cm\,s^{-1}$];
v_s, particle gravitational settling speed, $g\tau$ [$cm\,s^{-1}$];
V, fluid velocity within the boundary layer of a single cylindrical fiber in the direction normal to the wall [$cm\,s^{-1}$];
w, vapor concentration;
X, nondimensional coordinate parallel to the obstacle, equation (3.12);
Y, nondimensional coordinate normal to the obstacle, equation (3.15);
z, height normal to the rough plate [cm].

Greek symbols

Γ, gamma function;
δ_v, thickness of momentum boundary layer [cm];

* Present address: Department of Mechanical Engineering, Yale University, Box 2159 YS, New Haven, CT 06520, U.S.A.

ε, eddy diffusivity [$cm^2 s^{-1}$];
η, collection efficiency, defined in equation (3.4); also viscous length, equation (3.5);
μ, high Reynolds number particle deposition parameter, defined in equation (3.17);
ν, fluid kinematic viscosity [$cm^2 s^{-1}$];
τ, particle relaxation time, related to D by Einstein's formula $D = kT\tau/m_p$ where k is Boltzmann's constant, T the absolute temperature and m_p the particle mass [s];
Ψ, nondimensional particle deposition function, equations (3.22) and 3.28);
ω, deceleration parameter describing the inviscid velocity field close to the stagnation point (3.1) [s^{-1}].

1. INTRODUCTION

THERE is much interest in the rates at which pollutants (particles or gases) are transported from the atmosphere to the ground. Yet our understanding of the underlying phenomena is so limited that the recent review by Sehmel [1] concludes that the available experimental data show a scattering of three and four orders of magnitude for deposition velocities of particles and gases respectively. To reduce this uncertainty, we consider the problem of mass transfer from turbulent flows to a certain class of rough surface as an appropriate model for the atmosphere–ground interface. In this study, we make use of the considerable engineering literature on transport to rough surfaces.

Soon after Nikuradse's [2] experiments on turbulent flows over sand-roughened surfaces, the concept of the 'equivalent sand roughness' was introduced as a practical tool to correlate friction data. Since then, rough wall problems have been most commonly described from a macroscopic (or phenomenological) point of view: rather than studying surface microscopic structures and their relation to the flow field, engineers have tended to measure a single macroscopic overall property, the 'surface equivalent sand roughness' k_s. A number of authors have sought a more fundamental way to approach the problem, trying to relate the total drag (or heat and mass fluxes) observed on rough surfaces to the individual transport rates to each of the protruding elements. Indeed, the microscopic line of attack† is a most natural one: for instance, the fact that the friction coefficients on plates and channels are Reynolds numbers independent for fully rough flows (those in which the roughness elements penetrate into the fluid far beyond the viscous sublayer) is often explained by the dominance of the Reynolds-number-independent form of drag of individual protrusions over the total drag. Yet, when one makes a momentum (or mass) balance on the basis of this microscopic model, the results are often unsatisfactory. The early work of Schlichting [3], which is still one of the best examples of this approach, is characteristic of some of the frustrating aspects of the microscopic method. Schlichting measured friction coefficients for six different protrusion shapes at various concentrations, and compared the resulting individual drag coefficients of his roughness elements, extracted from the total drag of the rough plates, with the known values under isolated conditions. He obtained some qualitative agreement, but the inferred drag coefficients varied substantially as a function of roughness concentration (over an order of magnitude in some of the cases), showing larger friction factors than expected from the drag of individual protrusions for small densities, and smaller values for high concentrations of roughness elements. Unfortunately, 45 years later, in spite of some notable attempts [4] the situation has not improved much: we still lack a reliable method of predicting friction coefficients from the microscopic structure of rough surfaces. The fluid motion around those many obstacles with strong spatial inhomogeneities, very high turbulence intensities and large separated regions has been too complex to describe microscopically. The situation for the transport of vapors and heat to rough surfaces is similar. Attempts to relate the rate of mass transfer to single roughness elements with the total mass captured on the rough surface have lead to order of magnitude agreement but not to accurate predictions [5]. The complexity of the problem offers little hope of producing completely successful microscopic theories of transport phenomena to rough surfaces; however, the order of magnitude agreement achieved thus far suggests that our knowledge of transport efficiencies to single elements might be useful to correlate overall transport efficiencies to rough surfaces. Indeed, Yaglom and Kader [6] have succeeded in correlating a fairly large number of vapor and heat diffusion data to fully rough surfaces for the case of densely packed roughness elements of various forms. Although the physical model they used does not specifically incorporate single protrusion capture efficiencies, it is easily shown (Section 2) that the nondimensional group playing a major role in their correlation is precisely the Stanton number for mass or heat transfer to single roughness elements.

In this paper we show that the rate of mass transfer to fully rough surfaces is closely related to the 'single element capture efficiencies' for a more complex system than that studied by Yaglom and Kader [6], namely, the turbulent deposition of particles to grass. For this purpose we will first introduce the high Reynolds number form of Friedlander's [7] theory for the deposition of particles to solid obstacles by diffusion and interception, and use it to correlate the wind tunnel measurements of Chamberlain [8]. It will be seen that the available data collapse into a single curve when plotted in terms of the similarity variables suggested by the theory. The proposed correlation is

† From here on this more fundamental point of view will be called 'microscopic' as opposed to the macroscopic or phenomenological equivalent sand roughness approach.

successful over more than nine orders of magnitude for the nondimensional particle deposition velocity (even beyond the expected limits of validity), covering particle sizes from 32 to 0.08 μm and a range of friction velocities.

2. TRANSPORT OF VAPORS TO ROUGH SURFACES

2.1. *Introduction*

Many experimental and theoretical studies have been made of the turbulent transfer of heat and mass to rough surfaces in channels and tubes. Much of this work was reviewed by Yaglom and Kader [6]. They have been able to correlate an important subclass of the data in rather simple terms, and proposed a model for the hydrodynamic structure of the roughness sublayer which led them to an expression for the mass (heat) transfer resistance across this sublayer that agrees rather well with a large number of data for the case of closely packed 3-dim. roughness elements†. The model proposed predicts a sublayer transport resistance proportional to

$$h^{+1/2}(Pr^{2/3} - b') \tag{2.1}$$

where $h^+ = hu_*/\nu$ is the nondimensional form of the characteristic protrusion height h, u_* is the friction velocity for the turbulent flow, and ν is the fluid kinematic viscosity. Pr is the Prandtl number, or ratio between ν and the molecular diffusivity of heat (mass), and b' is a small constant. The model includes no dependence on shape and spacing between roughness elements because the data were not sufficient to assess systematically this effect and little was known of the hydrodynamic structure of the roughness sublayer. But this situation has changed recently, based primarily on fundamental studies of turbulent flows over rough surfaces at a very different scale, in the atmospheric boundary layer in and above plant canopies. The recent review of Raupach and Thom [10] has been an important step towards a synthesis between the engineering and the atmospheric scales. Raupach and Thom [10] do not cite previous studies at the engineering scale but they refer to their own remarkable wind tunnel-experiments [11] in which the hydrodynamic structure of the roughness sublayer is partially unveiled. Those data show a weak variation of the mean velocity within the roughness sublayer, which does not extrapolate to zero as the bottom wall is approached, contradicting the assumption of the Yaglom and Kader [6] model (Section 2.2). Thus, in Section 2.3, we shall introduce the alternative 'filtration model' (not new in the atmospheric literature [12]) for mass (heat) transfer, which will lead naturally to the Yaglom and Kader group $h^{+1/2}Pr^{2/3}$ governing the transfer resistance across the roughness sublayer. Our approach does not result in absolute predictions but provides certain correlation parameters; it may easily be extended to study the capture of particles including inertial and interception effects [13].

2.2. *The Yaglom and Kader model* [6]

The physical model which leads Yaglom and Kader to the successful expression (2.1) for the mass transfer resistance across the roughness sublayer was based on the early ideas of Levich [14]. Making a sound assumption on the form of the eddy viscosity coefficient, Levich integrated the streamwise momentum conservation equation assuming a constant value for the shear stress, and obtained the expression

$$u = u_* z/h \tag{2.2}$$

where z is the distance from the wall for the mean velocity within the roughness sublayer for the case of walls with small concentrations of protrusions. From equation (2.2), Levich [14] showed that the thickness of the boundary layer (at the wall, below the roughness elements) varies as $h^{+1/2}$, in agreement with equation (2.1). But for the closely packed roughness case considered by Yaglom and Kader, equation (2.2) is in clear disagreement with the data [11] which show that u changes weakly within the roughness sublayer. Even if a linear variation with z were compatible with experiments, u would not extrapolate to zero close to the wall (ref. [11], pp. 390–391) but to a value comparable to the velocity at $z = h$. Therefore equation (2.2) is not confirmed by experiments, and (as discussed by Levich [14]) both Levich's model and the Yaglom and Kader extensions of it are not applicable to densely packed roughness elements.

2.3. *The filtration model*

Much of the area available for heat and mass transport to walls covered with closely packed roughness elements is not at the bottom wall, but at the protrusions themselves. Since the convective motion is much more intense around them than at the bottom layer, a large fraction of the transfer of heat or matter would be expected to occur at the roughness elements. Accordingly, they may be viewed as heat or mass 'sinks' volumetrically distributed within the flow field, and the transport process may be modeled as routinely done in gas filtration [13]. Filtration models have been used previously to study the transport of heat and mass [12, 15], or momentum [10] within vegetation canopies. Here we show that the idea is also applicable at the much-smaller engineering scale studied by Levich, and provides a theoretical justification for Yaglom and Kader's successful correlation (2.1).

First, let us consider a single roughness element immersed in a stream with an imposed velocity field equal to the one prevailing in the roughness sublayer. Let us also assume that the vertical and horizontal dimensions of the object are comparable, of the order h. Then the fluid velocity around the protrusion is characterized by a Reynolds number of the order h^+,

† Although the agreement for 2-dim. roughness elements was much less satisfactory, Kader and Yaglom [9] have also found correlations valid for this type of roughness. Here we will be concerned only with the 3-dim. type, most often occurring in nature.

which for fully rough walls is much larger than unity [16]. Accordingly, one may use boundary layer theory to describe the transfer of matter and heat to the element, and the thickness of the momentum boundary layer δ_v near the protrusion leading edge is of the order of $h/h^{+1/2}$, much smaller than h. Thus, even if the free stream turbulence intensity is of order unity (based on forest, and also wind tunnel measurements [17]) the scale of the eddies is large compared to δ_v, and the initial boundary layer developing around the protrusion is laminar†. Accordingly, we may use the rather extensive literature for heat and mass transfer to solid bodies immersed in a fluid. (Indeed, the weak variation of μ with z makes it acceptable to use data from experiments at uniform upstream velocity.) Then we define a local capture efficiency or Stanton number for a single protrusion

$$\eta = \frac{j''}{u(z)w\rho} \tag{2.3}$$

based on the local mass flux j'', the mean incoming velocity $u(z)$ and w, the difference between the value of the condensing species concentration far from the obstacle and at the wall. (Provided the latter value is independent of z, this constant shift preserves the form of the mass conservation equation.) For convenience, at every surface strip at a height z, j'' is averaged horizontally and η is only a function of z. Now, given a rough surface with a density of individual roughness elements such that the mean area per unit volume available for deposition at a height z is $S(z)$, the mean effect of the roughness may be approximated by a mass sink

$$\left.\frac{dw}{dt}\right]_z = -\eta(z)\,u(z)\,S(z)\,w(z) \equiv -Kw. \tag{2.4}$$

If we adopt a turbulent diffusion coefficient ε and assume fully developed conditions (independent of x and y on the average) the mass conservation equation for the diffusing species may be written as

$$\frac{d}{dz}\left[(D+\varepsilon)\frac{dw}{dz}\right] = Kw \tag{2.5}$$

(D is the molecular diffusion coefficient in the mixture) with boundary conditions

$$w(h) = w_e \tag{2.6}$$

$$w(0) = 0. \tag{2.7}$$

Rather than solving equation (2.5) with a particular model for ε and K, it is convenient first to make some order of magnitude remarks: ε is of the order of

$$\varepsilon \sim hu_* \tag{2.8}$$

thus, much larger than D for gases (because $h^+ \gg 1$, $D/\nu \leqslant 1$) except near a bottom layer of thickness ν/u_*. Then, the only relevant nondimensional parameter entering the problem is

$$Q \equiv Kh/u_*. \tag{2.9}$$

But $Q = \eta uSh/u_* \simeq \eta Sh$, and for the most favorable case of a very dense packing of roughness elements, Sh is of the order of unity. Thus, in general, $Q < \eta$, and because for high h^+ the capture efficiency for vapors is small (as $h^{+1/2}$) the result is

$$Q \ll 1.$$

Accordingly, the concentration profile $w(z)$ is weakly modified by the sink (Kw) and, like $u(z)$, may be expected to vary weakly with z within the roughness sublayer. Thus, since the total mass flux to the protrusions is given from equation (2.5) by

$$j'' = \int_0^h \rho K w \, dz \tag{2.10}$$

we approximately have

$$j'' \sim \bar{K}\rho h w(h) \tag{2.11}$$

where $\bar{K}$ is a mean value of K in the region $0 < z < h$. This expression accounts only for the vapor collected on the roughness elements, not at the bottom wall, but the important point here is that the flux j'' is proportional to K and thus to the single protrusion capture efficiency. But for laminar diffusion at high Reynolds numbers, η is of the order of $Re^{-1/2}\,Pr^{-2/3}$: for instance, for a sphere [19]

$$\eta = 0.6\,Re^{-1/2}\,Pr^{-2/3} \tag{2.12}$$

while for a bed of spheres the behavior is identical, with a coefficient three times larger (1.82). Now, since Re is based on a characteristic length of the order of h and a characteristic velocity of the order u_*, it is itself of the order of h^+, and the mass transfer resistance across the roughness sublayer is

$$\frac{u_* w(h)}{j''} \sim \frac{u_*}{hS\eta U} \sim h^{+1/2}\,Pr^{2/3}\,\frac{1}{hS} \tag{2.13}$$

where $hS \sim 1$ for closely packed roughness elements. Thus we obtain a roughness sublayer resistance proportional to $h^{+1/2}\,Pr^{2/3}$. This expression differs from equation (2.1) in that it involves the group $Pr^{2/3}$ rather than $(Pr^{2/3} - b')$ as in the Yaglom and Kader formula. But, given the small value of b' adopted by those authors, ($b' = 0.2$) the difference is small.

In conclusion, the filtration model predicts a mass transfer rate proportional to the single element capture efficiency η, which in the region of diffusive deposition

† A similar phenomenon occurs for the laminar boundary layer developing around an airplane wing in the turbulent atmosphere, or around a gas turbine blade in the highly turbulent stream of gases coming from the combustion chamber. The free stream turbulence has an effect on the boundary layer development around the protrusion because it precipitates its transition to turbulence, but this influence is only moderately important, because the transfer rates in the laminar and turbulent portions are comparable (ref. [16], Fig. 12.18). The direct effect of free stream turbulence on the heat transfer to the laminar part amounts to an 80% enhancement (ref. [18] Figs. 4 and 18) for a cylinder in cross flow, and free stream turbulence levels above 2%.

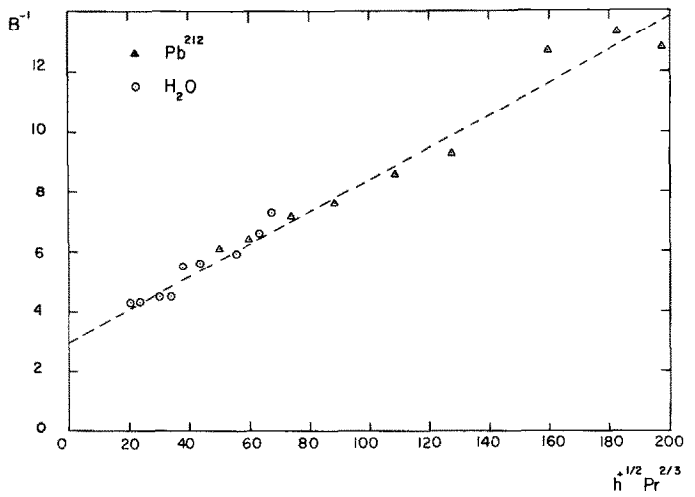

FIG. 1(a). Mass transfer resistance coefficient

$$B^{-1}\left(\equiv \frac{u_*}{v_g} - \frac{u(h)}{u_*}\right)$$

in the roughness sublayer of artificial grass. Data from ref. [5] for deposition of Pb^{212} and evaporation of water. The single element collection efficiency group $(Pr^{2/3}\, h^{+1/2})^{-1}$ correlates the data well.

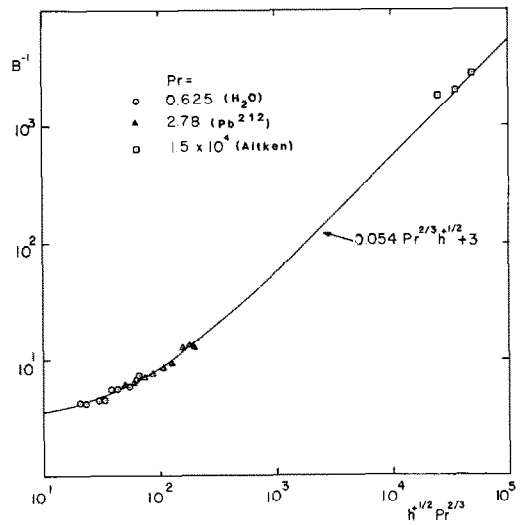

FIG. 1(b). Extension of Fig. 1(a) to include the data from [8] on Aitken nuclei deposition to the same surface with artificial grass.

has the same form as Yaglom and Kader's successful correlation. However, the agreement is qualitative because our model yields

$$\frac{\rho w(h) u_*}{j''} = G h^{+1/2}\, Pr^{2/3} \tag{2.14}$$

with G depending linearly on the concentration of roughness elements, while Yaglom and Kader obtain

$$\frac{\rho w(h) u_*}{j''} = 0.55\, h^{+1/2}\,(Pr^{2/3} - 0.2) + 9.5 \tag{2.15}$$

which not only shows a large constant shift of 9.5 over our prediction, but where the constant 0.55 is independent of the density of protrusions (rather than linear) at large densities. Furthermore, the values of the constant G which we infer from equations (2.11) and (2.12) based on conditions reported by Chamberlain [20] for two different walls roughened with hemispherical elements are close to 1 and 3 respectively comparing poorly with the experimental value 0.55. On the other hand, the value $G = 0.55$ given in ref. [6] is far from being universal. This may be seen for instance in Fig. 1(a) in which we plot mass transfer resistance measurements to artificial grass from [5]. Although the data for both, H_2O and Pb^{212} (with values of Pr of 0.625 and 2.78 respectively [5]) fall approximately on a single curve when plotted versus the group $h^{+1/2}\, Pr^{2/3}$, the corresponding slope is now $G = 0.054$, an order of magnitude smaller than would be expected from equation (2.15). This is not surprising because the range of application of the Yaglom and Kader correlation is limited to protrusions with similar heights and widths. Our model is not so constrained because an equation of the type (2.12) applies to bodies such as spheres or cylinders provided that the Reynolds number is based on the transverse dimension R rather than k. The use of R leaves the conclusion of [6] unchanged since $R \simeq h$, but alters the application to Chamberlain's artificial grass for which the ratio h/R was 15. Indeed, in terms of the variable

$$\left(\frac{R v_*}{\nu}\right)^{1/2} Pr^{2/3} \tag{2.16}$$

suggested by our model, the slope of Fig. 1(a) increases (by a factor of $\sqrt{15}$) to become 0.21, much closer to the value of 0.55 found by Yaglom and Kader. Thus, consistent with our approach, it is appropriate to use the group (2.16) rather than $h^{+1/2}\, Pr^{2/3}$ in future work.

Our retention of the latter factor in Figs. 1(a) and (b) serves to facilitate comparison with ref. [6].

The range of values of h^+ covered in Fig. 1(a) is considerable, but only two values of Pr are involved, limiting the validity of our conclusions to molecular diffusion in gases (the same restriction applies to the data studied by [6]). Fortunately, Chamberlain [8] has also measured the rate of deposition of Aitken nuclei (with $Pr = 1.5 \times 10^4$) to the same artificial grass surface. These data are plotted in Fig. 1 (b) together with the vapor transport data, and fall along the same line $B^{-1} = 3 + 0.054\, h^{+1/2}\, Pr^{2/3}$ which passes through the vapor diffusion data of Fig. 1(a). This provides the first indication of the wide range of validity of the filtration model predictions, though it would be interesting to test it also for the case of large Prandtl number diffusion in liquids. The momentum transfer properties for this type of rough surfaces are also unusual: the equivalent sand roughness k_s is some ten times greater than the actual height h for Chamberlain's artificial grass, in contrast with the usual behavior for surfaces with densely packed bluff elements where h and k_s are close to each other. In most engineering situations, with sparsely distributed roughness, k_s is around 30 times smaller than h.

3. TRANSPORT OF PARTICLES TO ROUGH SURFACES

3.1. *Introduction*

The validity of equation (2.11) relating the total mass flux to a rough wall with the single element collection efficiency η is not, in principle, restricted to diffusional deposition; it is then worth testing its usefulness when other mechanisms such as inertia, interception, electrostatic or gravitational forces, etc. are present.

Some of the best data on mass transfer to rough surfaces have been obtained by Chamberlain [5, 8, 20] both in the field and the wind tunnel, over a variety of roughness elements (wavy, bluff, or grasslike), for vapor and particle deposition, and for a wide range of friction velocities. Furthermore, Chamberlain's [20] diffusion measurements to surfaces with ordered roughness elements played a major role in the development of the successful correlation (2.15) for vapor deposition, so it is natural to test a new model of particle deposition to surfaces with ordered protrusions against the data in [20]. Besides their precision and the wide margin of parameters covered, those data have the additional interest of applying not only to grassy land, but to a variety of cultivated or natural plant canopies.

From the theoretical side, most often interception effects start affecting particle diffusion before inertia sets in. Besides, the theory of particle deposition on single fibers by the simultaneous action of diffusion and interception is well developed and agrees satisfactorily with low Reynolds number experiments [7, 13, 21]. Therefore it is appropriate to adapt Friedlander's [7] diffusion and interception treatment to the high Reynolds number conditions prevailing in the experiments, and to compare it with the data. This program is developed in the following subsections (3.2) and (3.3).

3.2. *Single element particle capture by diffusion and interception at large Reynolds numbers*

For simplicity we will choose a 2-dim. geometry corresponding to the flow normal to a bluff body of arbitrary shape. The origin of coordinates is taken at the stagnation point, and the y axis is normal to the surface at every point, y being zero at the surface. Generalization to 3-dim. geometries is trivial, and leaves the main conclusions [equation (3.22)] unchanged.

The high Reynolds number velocity field in the inviscid region close to the stagnation point is given by Schlichting ref. [16], pp. 87–89)

$$(U, V) = (\omega x, -\omega y) \tag{3.1}$$

and within the viscous layer

$$U = \omega x f'(\eta) \tag{3.2}$$

$$V = -(\nu\omega)^{1/2} f(\eta) \tag{3.3}$$

where η is the nondimensional viscous length

$$\eta = y(\omega/\nu)^{1/2} \tag{3.4}$$

and the near wall behavior of the function f is

$$\left.\begin{aligned} f(\eta) &= \tfrac{1}{2}k\eta^2 \\ f'(\eta) &= k\eta \end{aligned}\right\} \eta \ll 1 \qquad \begin{matrix} (3.5) \\ (3.6) \end{matrix}$$

with

$$k = f''(0) = 1.2326. \tag{3.7}$$

Therefore, sufficiently close to the stagnation point

$$U = \omega x k\eta, \tag{3.8}$$

$$V = -\tfrac{1}{2}(\nu\omega)^{1/2} k\eta^2. \tag{3.9}$$

In the region close to the wall, provided the flow has not separated and before transition to turbulence, equations (3.8) and (3.9) can be generalized away from the stagnation point to give

$$U = \omega R K(X)\eta \tag{3.10}$$

$$V = -\tfrac{1}{2}(\nu\omega)^{1/2} K'(X)\eta^2 \tag{3.11}$$

where we have nondimensionalized x with the obstacle characteristic length R

$$X = x/R \tag{3.12}$$

and also

$$K' = \frac{dK}{dX}. \tag{3.13}$$

For large Reynolds numbers, the function K depends on the particular shape of the obstacle, and can be calculated by standard methods of boundary layer theory ref. [16], p. 154). Then, the equation expressing conservation of the particle density n is, in the boundary layer approximation,

$$-D\frac{\partial^2 n}{\partial y^2}+\omega K\eta\frac{\partial n}{\partial X}-\tfrac{1}{2}K'(\nu\omega)^{1/2}\frac{\partial n}{\partial y}=0 \quad (3.14)$$

and defining the nondimensional vertical length based on the particle radius r_p,

$$Y = y/r_p \quad (3.15)$$

it becomes

$$\frac{\mu^{-3}}{3}\frac{\partial^2 n}{\partial Y^2}-2KY\frac{\partial n}{\partial X}+K'Y^2\frac{\partial n}{\partial Y}=0 \quad (3.16)$$

with

$$\mu^3 \equiv \frac{1}{6}\frac{\nu}{D}r_p^3(\omega/\nu)^{3/2}. \quad (3.17)$$

This equation must be solved with the standard diffusion–interception boundary conditions [7]

$$n = n_e \quad \text{for } Y \to \infty, \quad (3.18)$$

$$n = 0 \quad \text{at } Y = 1. \quad (3.19)$$

The solution for any given obstacle [$K(X)$ fixed] is

$$n/n_e = F(X, Y, \mu) \quad (3.20)$$

and the average mass flux to the obstacle is

$$j'' \equiv \frac{\oint D\frac{\partial n}{\partial y}\Big]_{r_p}\mathrm{d}x}{\oint \mathrm{d}x} = \frac{Dn_e}{r_p}\frac{\oint \frac{\partial F}{\partial Y}\Big]_1 \mathrm{d}X}{\oint \mathrm{d}X} \quad (3.21)$$

where by the symbol $\oint$ we mean integration along the cylinder perimeter. Then, the group $j''r_p/(Dn_e)$ depends only on the parameter μ

$$\frac{j''r_p}{Dn_e} = \Psi(\mu). \quad (3.22)$$

Equation (3.22) generalizes Friedlander's [7] result to the large Reynolds number case. Notice that the deposition variable $j''r_p/(n_eD)$ obtained here is identical with its low Reynolds number counterpart. Also, realizing that the Reynolds number in our case is

$$Re \sim \omega R^2/\nu \quad (3.23)$$

we have

$$\mu \sim \frac{r_p}{R}Re^{1/2}(\nu/D)^{1/3} \quad (3.24)$$

which is related with the corresponding low Reynolds number parameter

$$(\mu)_{Re\ll 1} \sim (r_p/R)\,Re^{1/3}(\nu/D)^{1/3} \quad (3.25)$$

through the weakly-varying factor $Re^{1/6}$

$$\mu \sim Re^{1/6}(\mu)_{Re\ll 1}. \quad (3.26)$$

Interestingly enough, the new parameter μ has been used previously to correlate filtration efficiencies on purely empirical grounds [22, 21].

3.3. *Comparison with experiments*

Figure 2(a) shows the data of Chamberlain [8] on particle deposition over artificial grass using the similarity variables suggested by the above theory,

$$j''r_p/(Dn_e) \text{ vs } \frac{2r_p}{R}Re^{1/2}(\nu/D)^{1/3}.$$

We have used the reported particle deposition velocity v_g in place of j''/n_e. The characteristic length R chosen is the transverse dimension of the strips forming the artificial grass elements, $R = 0.5$ cm. For the Reynolds number we have adopted the value $Re = 2.3u_*R/\nu$ based on the mean streamwise velocity $2.3u_*$ measured at the top of the simulated blades [5] and D has been calculated from equations 2, 3, 4 and 5 of ref. [7]. It is clear that all the data collapse into a single curve over the wide range of parameters explored by Chamberlain: the data include six different particle sizes (32, 19, 5, 2, 1 and 0.08 μm diameter) at three values of the friction velocity (140, 70, and 35 cm s^{-1}), as well as six more points with lycopodium spores (32 μm dia. at six

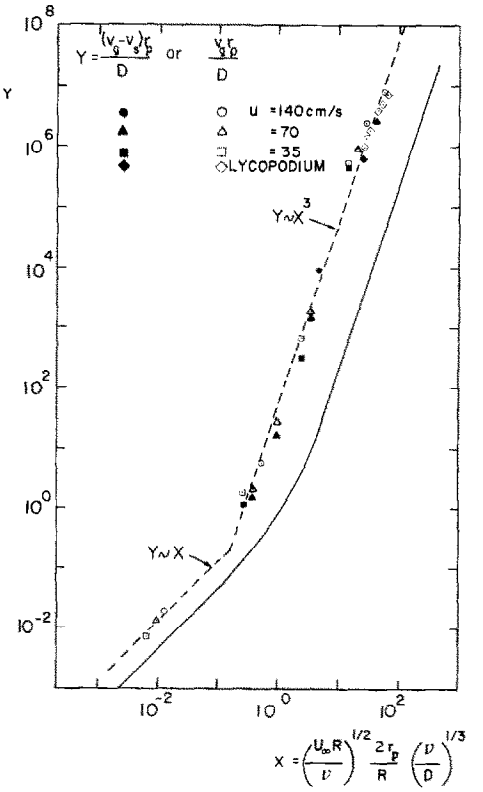

FIG. 2(a). Nondimensional particle deposition velocity to artificial grass as a function of the deposition parameter. Data from ref. [8], corrected (black symbols) and uncorrected (white symbols) for gravitational settling. Two broken lines (---) with slopes 3 and 1 (corresponding to the interception and diffusion asymptotic regions) are drawn through the data. The solid line (——) shows, as a reference, the single fiber collection efficiency at the stagnation point of an infinite strip normal to the unseparated potential flow. $U_\infty = 2.3u_*$, R = 0.5 cm = strip width. The lycopodium experiments (◇) were carried out over a wider range of values of u_* than the other particles.

different friction velocities (146, 120, 84, 73, 44 and 28 cm s^{-1}). For comparison purposes, we have also drawn the theoretical curve corresponding to the deposition to a single fiber at the stagnation point where the function $K(X)$ is

$$K(X) = kX \tag{3.27}$$

and X is close to zero. Then the function Ψ in equation (3.22) can be obtained analytically [7] to yield

$$\frac{j''r_p}{Dn_e} = \Psi(\mu) = \frac{\exp(-\mu^3)}{\int_1^t \exp(-\mu^3\xi^3)d\xi}. \tag{3.28}$$

The asymptotic behavior of $\Psi(\mu)$ is (in terms of the gamma function Γ)

$$\mu \to 0,\ \Psi \to \mu/\Gamma(4/3) \quad \text{(diffusional limit)} \tag{3.29}$$

$$\mu \to \infty,\ \Psi \to 3\mu^3 \quad \text{(interception limit)} \tag{3.30}$$

while in the region where μ is of order unity, the transition can be described very accurately by summing a series

$$\Psi(\mu) = \mu\exp(-\mu^3)\left[\Gamma(4/3) - \mu\sum_{m=0}^{t}\frac{(-\mu)^{3m}}{(3m+1)m!}\right]^{-1} \tag{3.31}$$

The asymptotic behavior for large μ requires a slope of three in a log–log plot, which is accurately followed by the data. The expected slope for lower values of μ is unity; this is also followed reasonably well, though we cannot be certain because only three of Chamberlain's points fall in this region, all of them for a single particle size, which was measured with less precision than the remaining points in the data. A quantitative comparison requires relating the deceleration rate parameter ω (entering into the definition of μ) with the known variables U_∞ ($= 2.3u_*$) and R appearing in our plot. For the potential flow around an obstacle one generally has

$$\omega = bU_\infty/R \tag{3.32}$$

where the constant b depends on the body geometry. A number of values are reported by Fuchs [23]. We have selected $b = 2$, corresponding to a flat strip normal to the incident (unseparated) stream, though any other value of order unity would be equally reasonable because the flow is not potential, normal to the strip, nor unseparated.

In spite of the considerable shift between the data and the reference theoretical curve, this qualitative agreement over more than nine orders of magnitude of the deposition variable is impressive. Moreover, the vertical shift between theory and data is significantly less than shown in the figure if we consider that:

(1) The theoretical line represents the single blade efficiency while the data refer to total surface deposition. The former should therefore be increased by a factor of 4.2, the surface area of the grass per unit horizontal area. [Based on data for cylinders, where the back separated face contributes roughly as much as the front laminar region for heat transfer (ref. [16], Fig. 12.18), we have assumed that the front and the back sides of the strips are equally efficient mass sinks.]

(2) The theoretical line ignores free stream turbulence effects, which are known to enhance diffusive deposition rates [18]. This effect cannot be predicted in the interception region because no data are available, and no existing theory can explain the observed free stream turbulence effects, not even in the relatively simpler diffusion region [18]. Nonetheless, interception deposition increases as the 3/2 power of the instantaneous free stream velocity U_∞ whose mean value is certainly larger than $U_\infty^{3/2}$. Therefore, this effect alone should account for an increase by a factor of 2 or 3 in interception at the large turbulence levels present. If these corrections for area and turbulence are taken into account, the predicted deposition velocity based on single element theory falls about one order of magnitude below the data in Fig. 1(a).

Figure 2(b) expands Fig. 2(a) to include the vapor deposition data of [5], previously shown in Figs. 1(a) and (b). This extends the region of validity of the correlation to fifteen orders of magnitude of the group $(v_g r_p/D)$, from relatively large particles to molecular dimensions. We have used for r_p the values 2.66×10^{-8} and 5.62×10^{-8} cm for H_2O and Pb^{212} respectively, based on the Chapman–Enskog expression for the diffusion coefficients of perfectly reflecting hard spheres. This form of representation is not the most appropriate for the diffusion of vapors, as the data do not strictly fall into a single curve for values of $v_g r_p/D$ less than 10^{-5}, but they nearly do so, and the figure shows the gradual transition from vapor to particle behavior.

As a reference, we also plot the data of Chamberlain [8] in Fig. 3 in the more standard form, particle deposition velocity v_g vs particle diameter d_p. Only the data for $u_* = 70$ cm s^{-1} are shown, as the other behave in a similar way. The characteristic minimum in the submicron range is clear, though with only one point in the diffusion region. Note that the deposition velocities for lycopodium and ragweed particles are very close to each other (for all three values of u_*). This anomaly is also visible in Fig. 2(a), where the three ragweed data points fall systematically to the left of the remaining points. Ragweed thus behaves as it it were effectively larger than it really is, in qualitative agreement with Chamberlain's observation [8] that "the pollen grains are spherical, but the surfaces are covered with warts a few microns in height" These "warts" would not affect inertial or diffusive effects significantly, but would certainly modify the effective diameter of the particles for interception. Therefore, the "ragweed shift" is consistent with the interception mechanism.

3.4. *Inertial effects*

Another interesting aspect of the proposed correlation is that it works beyond the expected limits of validity, as significant inertial effects would be expected

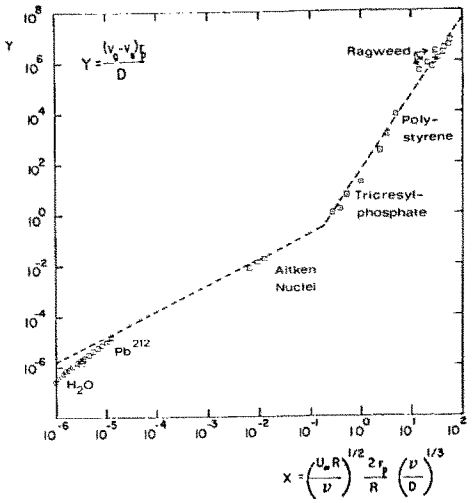

FIG. 2(b). Extension of Fig. 1(a) to include the data from ref. [5] on vapor diffusion to artificial grass. Note the smooth transition from gas to particle deposition behavior.

for the two larger particle sizes. The critical Stokes number marking the onset of inertia corresponds to $\omega\tau = \frac{1}{4}$, τ being the particle relaxation time. But for the case of lycopodium spores at $u_* = 140\,\mathrm{cm\,s^{-1}}$, we obtain

$$\omega\tau = b\frac{U_x\tau}{R} = 2.5$$

(again we have taken $b = 2$, $U_x = 2.3u_*$, $R = 0.5\,\mathrm{cm}$),

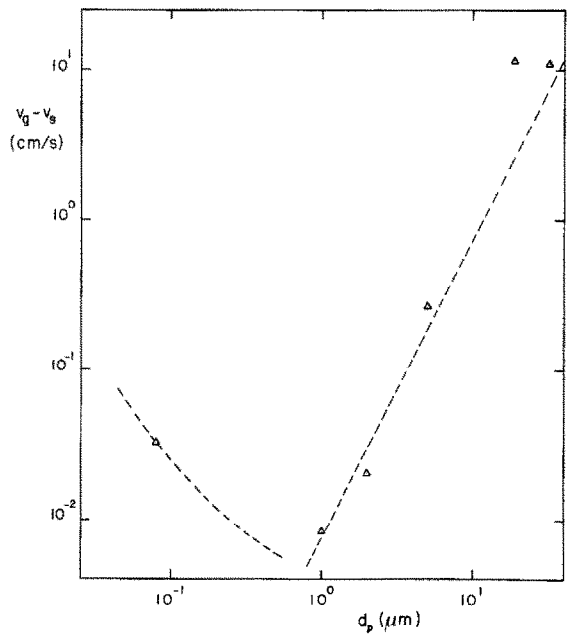

FIG. 3. Particle deposition velocity v_g as a function of particle diameter d_p. Data for artificial grass [8]; $u_* = 70\,\mathrm{cm\,s^{-1}}$. Broken lines correspond to the asymptotic behavior: $v_g \sim (D/\nu)^{2/3}$; $v_g \sim d_p^2$.

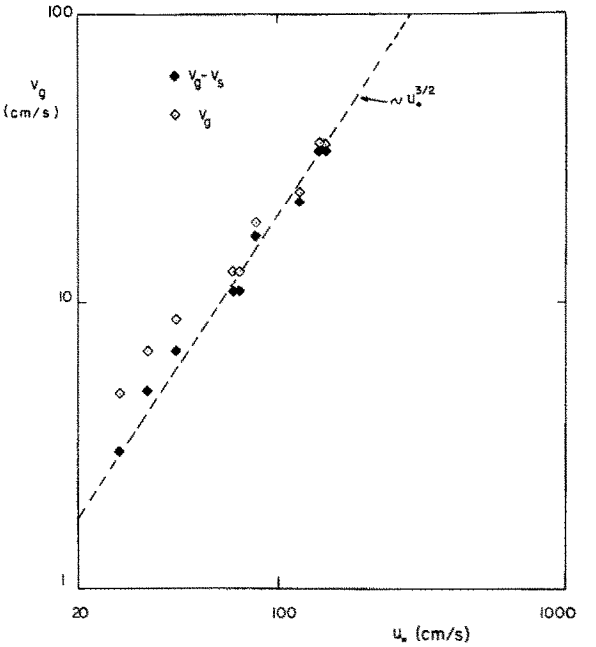

FIG. 4. Particle deposition velocity v_g corrected (◆) and uncorrected (◇) for the gravitational settling speed v_s, as a function of the friction velocity u_*. Data for lycopodium particles [8]. The broken line drawn through the data shows the 3/2 power dependence expected from interception.

which is well supercritical. Yet no inertial effects are seen from the data: Figure 4 shows a plot of the particle deposition velocity (corrected and uncorrected for the gravitational settling) against the friction velocity, and it may be seen that the dependence is

$$v_g \sim u_*^{3/2}$$

as expected from interception. The inertial deposition rates should depend more strongly on u_*. This fact may be due to bounce off, to the channeling of the stream between the different strips, to the high interception deposition rates which overshadow the inertial contribution, or possibly to all these phenomena acting together. In any case, it is unlikely that the correlation will remain valid for higher particle sizes or wind velocities.

4. CONCLUSIONS AND FURTHER WORK

Rates of transport of heat and mass to rough surfaces are related to the transport rates to single roughness elements. An exact relationship was not found but an approximate analysis suggests that rough wall deposition data might be successfully correlated using parameters borrowed from single element deposition theories, and we have shown that this is the case for vapor and particle transport. For the case of vapors, this can be demonstrated by noticing that the group $Pr^{2/3}\ h^{+1/2}$, used previously to correlate a considerable number of heat transfer data, is directly related to the high Reynolds number heat transfer coefficient of single elements. For the case of particles,

we have developed a theory of deposition by diffusion and interception at high Reynolds numbers, consistent with the correlation principle when compared with data for particle capture by artificial grass: those data fall into a single curve when plotted in terms of the nondimensional variables suggested by the theory, and also show the same asymptotic behavior expected from single element capture in both the diffusion and the interception range. Surprisingly, the correlation holds beyond the expected limits of validity, in the region where we would expect considerable inertial effects. The observed capture rates are more than an order of magnitude higher than calculated from single element theory possibly due to the neglect of the high turbulence intensities within the roughness region. The dominant role played by the interception effect seems nonetheless well established for particle sizes from 1 μm to 20 or 30 μm. This result, if confirmed more generally, would permit approximate predictions of particle deposition velocities over the wide interception region in terms of a single constant C characteristic of each type of surface

$$v_g = v_s + Cu_*^{3/2} r_p^2. \qquad (4.1)$$

The mechanism of deposition of large ($d_p > 1\ \mu$m) particles to such rough surfaces differs significantly from the mechanism for transport to smooth surfaces [24]. For smooth surfaces, particle transport occurs by turbulent diffusion from the gas mainstream; the final deposition occurs by an inertial mechanism. For rough surfaces, particle transport from the gas mainstream into the roughness elements also occurs by turbulent diffusion. However, the final deposition takes place by filtration in the roughness elements; for the range of variables reported here, the interception mechanism was dominant.

The present work has dealt only with fully rough surfaces. A natural extension with promising engineering applications would be to study the hydrodynamically smooth limit. In this case, the roughness elements are small compared to the thickness of the viscous sublayer and a significant increase in particle capture is achieved at no cost in pressure drop [25]. Under these circumstances, the filtration model should be expected to work also, although the flow around the protrusions would be characterized by a small value of the Reynolds number.

Acknowledgements—We wish to thank Dr A. C. Chamberlain and Dr C. I. Davidson for their helpful comments on the manuscript. This work was supported in part by EPA Grant CR-807864-01. The contents do not necessarily reflect the views and policies of the Environmental Protection Agency.

REFERENCES

1. G. Sehmel, Particle and gas dry deposition: a review, *Atmos. Environ.* **14,** 983–1012 (1980).
2. J. Nikuradse, Laws of flow in rough pipes, NACA TM-1292 (1950).
3. H. Schlichting, Experimental investigations on the problem of surface roughness, NACA-TM 823 (1937).
4. M. J. Lewis, An elementary analysis for predicting the momentum- and heat-transfer characteristics of a hydraulically rough surface, *Trans. Am. Soc. Mech. Engrs, Series C, J. Heat Transfer* **97,** 249 (1975).
5. A. C. Chamberlain, Transport of gases to and from grass-like surfaces, *Proc. R. Soc.* **A290,** 236–265 (1966); J. Shreffler, *Appl. Met.* **15,** 744–46 (1976) and Brutsaert, *Boundary-Layer Metereol* **16,** 365–88 (1979).
6. A. M. Yaglom and B. A. Kader, Heat and mass transfer between a rough wall and turbulent fluid at high Reynolds and Peclet numbers, *J. Fluid Mech.* **62,** 601–623 (1974).
7. S. K. Friedlander, Particle diffusion in low speed flows, *J. Colloid Interface Sci.* **23,** 157–164 (1967).
8. A. C. Chamberlain, Transport of lycopodium spores and other small particles to rough surfaces, *Proc. R. Soc.* **A296,** 45–70 (1966).
9. B. A. Kader and A. M. Yaglom, Heat and mass transfer from a wall with parallel roughness ridges, *Int. J. Heat Mass Transfer* **20,** 345–357 (1977).
10. M. R. Raupach and A. S. Thom, Turbulence in and above plant canopies, *Ann. Rev. Fluid Mech.* **13,** 97–129 (1981).
11. M. R. Raupach, A. S. Thom and I. Edwards, A wind tunnel study of turbulent flow close to regularly arrayed rough surfaces, *Boundary-Layer Metereol.* **18,** 373–397 (1980).
12. C. I. Davidson and S. K. Friedlander, A filtration model for aerosol dry deposition: application to trace metal deposition from the atmosphere, *J. Geophys. Res.* **83,** 2343–2352 (1978).
13. S. K. Friedlander, *Smoke, Dust and Haze.* John Wiley, New York (1977).
14. V. G. Levich, *Physicochemical Hydrodynamics,* Section 30. Prentice–Hall, New Jersey (1967).
15. W. G. N. Slinn, Predictions for particle deposition to vegetative canopies, submitted to *Atmos. Environ.* (1980); W. G. N. Slinn, *Water, Air and Soil Pollution* **7,** 513–543 (1977), and D. H. Bache, *Atmos. Environ.* **13,** 1681–1687 (1979).
16. H. Schlichting, *Boundary Layer Theory,* 6th edn. McGraw–Hill, New York (1968).
17. M. M. Pimenta, R. J. Moffat and W. M. Kays, The turbulent boundary layer: an experimental study of the transport of momentum and heat with the effect of roughness, Rep. HMT-21, Dept. of Mech. Eng., Stanford University (1975).
18. J. Kestin, The effect of free stream turbulence on heat transfer rates in *Advances in Heat Transfer,* Vol. 3, pp. 1–33. Academic Press, New York (1966).
19. R. B. Bird, W. E. Stewart, and E. N. Lightfoot, *Transport Phenomena,* p. 409. John Wiley, New York (1960).
20. A. C. Chamberlain, Transport of gases to and from surfaces with bluff and wave-like roughness elements, *Q. J. Royal Met. Soc.* **94,** 318–332 (1968).
21. K. W. Lee, Filtration of submicron aerosols by fibrous filters, Doctoral thesis, Dept. Mech. Eng., University of Minnesota, Minneapolis (1977).
22. S. K. Friedlander, Theory of aerosol filtration, *Ind. Engng Chem.* **50,** 1161–1164 (1958).
23. N. A. Fuchs, *The Mechanics of Aerosols,* p. 169. Pergamon Press, New York (1964).
24. S. K. Friedlander and H. F. Johnstone, Deposition of suspended particles from turbulent gas streams, *Ind. Engng Chem.* **49,** 1151–1156 (1957).
25. A. C. Wells and A. C. Chamberlain, Transport of small particles to vertical surfaces, *Br. J. Appl. Phys.* **18,** 1793–1799 (1967).

DEPOT D'AEROSOL ET DE GAZ SUR LES SURFACES PLEINEMENT RUGUEUSES: MODELE DE FILTRATION POUR DES ELEMENTS EN FORME D'AILETTE

Résumé—Des flux de particules et de gaz transportés sur les surfaces rugueuses par des écoulements turbulents peuvent être reliés à des efficacités de collecte des éléments individuels de rugosité. Le transport sur les surfaces pleinement rugueuses est si rapide que la concentration (moyenne) est proche d'une constante entre le coeur de l'écoulement et la couche rugueuse et le caractère limitant le flux est le dépot sur les éléments rugueux. Des expressions pour les flux déposés peuvent être obtenues en utilisant la théorie de la filtration modifiée pour tenir compte des grands nombres de Reynolds autour des éléments. Des données de la littérature sur le transfert de particules et de gaz à des plaquettes de gazon artificiel peuvent être représentées en utilisant des variables adimensionnelles de la théorie de la filtration. La formule est satisfaisante sur plus de neuf ordre de grandeur de la variable de dépot et elle montre des formes limites convenant aux domaines des petites et des grandes dimensions de particules.

DIE ANLAGERUNG VON AEROSOLEN UND GASEN AN RAUHIGKEITSFLÄCHEN: EIN FILTRATIONSMODELL FÜR HALMFÖRMIGE ELEMENTE

Zusammenfassung—Die Geschwindigkeiten des Teilchen- und Gastransports aus turbulenten Strömungen an Rauhigkeitsflächen lassen sich mit den Auffangwirkungsgraden der einzelnen Rauhigkeitselemente in Verbindung bringen. Die Bewegung zur Rauhigkeitsoberfläche hin verläuft schnell, so daß die (mittlere) Konzentration zwischen Hauptströmung und Rauhigkeitsschicht fast konstant ist und die Bewegungsgeschwindigkeit durch die Anlagerung an die Rauhigkeitselemente begrenzt wird. Aus der Filtrationstheorie können Ausdrücke für die Anlagerungsgeschwindigkeit abgeleitet werden, die jedoch modifiziert werden müssen, um die hohe Reynolds-Zahl der Strömung an den Elementen zu berücksichtigen. Aus der Literatur können Daten über die Teilchen- und Gasbewegung an künstlichen Grashalmen ausgewertet werden, wobei dimensionslose Größen aus der Filtrationstheorie eingesetzt werden können. Die Korrelation ist über mehr als neun Größenordnungen der Variablen, die die Anlagerung bestimmt, zufriedenstellend und zeigt richtige Grenzwerte in den kleinen und großen Teilchengrößenbereichen.

ОСАЖДЕНИЕ АЭРОЗОЛЯ И ГАЗА НА ШЕРОХОВАТЫХ ПОВЕРХНОСТЯХ. ФИЛЬТРАЦИОННАЯ МОДЕЛЬ ДЛЯ ЭЛЕМЕНТОВ В ФОРМЕ УЗКИХ ПЛАСТИН

Аннотация—Скорость переноса частиц и газа из турбулентного потока к шероховатым поверхностям можно связать с коэффициентами их захвата отдельными элементами шероховатости. Перенос частиц и газа к полностью шероховатым поверхностям происходит настолько быстро, что их (средняя) концентрация оказывается почти постоянной во всей области от основного потока до слоя шероховатости. Скорость переноса замедляется в стадии осаждения частиц на элементах шероховатости. Интенсивность осаждения можно описать с помощью фильтрационной теории, учитывающей большие числа Рейнольдса при обтекании элементов потоком. Данные, опубликованные в ряде работ для искусственной травы, можно обобщить с помощью безразмерных переменных фильтрационной теории. Обобщающая зависимость удовлетворительно, в диапазоне шириной более девяти порядков, описывает величину осаждения. Кроме того, она правильно ведет себя в предельных случаях больших и малых частиц.